Paper 24

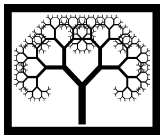

©Civil-Comp Press, 2012
Proceedings of the Eleventh International Conference
on Computational Structures Technology,
B.H.V. Topping, (Editor),
Civil-Comp Press, Stirlingshire, Scotland

A Hysteretic Displacement Based Fibre Beam Element

I.A. Gkimousis and V.K. Koumousis
Institute of Structural Analysis & Aseismic Research
National Technical University of Athens, Greece

Abstract

Distributed plasticity elements have been proved very efficient in predicting the response of structures under severe loading. In this paper a new displacement based fibre beam element in which hysteresis is treated explicitly is proposed. The stress-strain relation of each fibre is considered on the basis of Bouc-Wen model. Numerical integration of stresses at both cross sectional and elemental level results the internal nodal forces which are expressed in a form that separates the elastic and hysteretic component. The elastic part forms the global stiffness matrix of the structure, which remains constant throughout the entire analysis, while hysteretic nodal forces represent the non-linear behaviour and have to be updated at every time step. The updated total hysteretic force vector along the degrees of freedom of the structure is subtracted from the external load vector and the global equations of motion are solved numerically while their left hand side is maintained constant. Numerical examples are presented which verify the validity of the method and its capability and efficiency to yield accurate results.

Keywords: distributed plasticity frame element, fibre discretization, displacement based method, hysteresis, Bouc-Wen model, dynamic non-linear analysis.

1 Introduction

Recent advances in the field of performance based earthquake engineering have increased the demand of reliable simulation of structures forced to the inelastic regime under severe earthquakes. Hence, accurate models that incorporate plasticity and the inherent hysteretic behaviour in a computationally efficient way are needed. In this respect, realistic material behaviour has to be taken into account, as degradation effects appear in cycling loading and need to be addressed properly.

Finite element models for the elastoplastic analysis of frame structures can be divided in two main categories i.e., the concentrated and distributed plasticity models. In the first, plasticity is expressed in stress resultant terms and is anticipated to develop in predefined regions at the element's ends, forming the so called plastic hinges. In these areas rotational springs are used to model a non-linear moment-curvature behaviour. The parallel model by Clough et al. [1] that was later modified by Giberson [2] to account for stiffness degradation and strength deterioration is frequently utilized among others. Generally, these models depend on a number of parameters that need to be predefined, influencing considerably the structure's response. The second category corresponds to the distributed plasticity elements that monitor plasticity in more than two selected regions inside the element's length. These control sections are described by constitutive relations of classic plasticity in terms of stress resultants, or they are subdivided in longitudinal fibres representing a uniaxial stress-strain law [3]. The first elements of this category were based on the classical finite elements method (Bathe [4]) where the displacement field along the element is expressed with cubic polynomials. This methodology describes only constant axial force and linear curvature, which is not accurate in the plastic region where curvature is distributed non-linearly along the element. Consequently, inner nodes have to be introduced in the element to increase accuracy which in turn increases the computational cost. To address this problem, force based models have been proposed that interpolate nodal forces inside the element maintaining equilibrium. The thorough investigation of these models, in the general framework of the direct stiffness method following a standard non-linear finite element procedure, was performed by Spacone et al. [5]. They suggested an iterative procedure under constant displacements for the element state determination establishing compatibility. Later, Neuenhofer and Filippou [6] showed that elemental iterations are not necessary as the element stresses gradually converge while the whole structure is in equilibrium. The weak point of the force based elements is that they produce unrealistic behavior in softening-strain cases as they result different elemental responses for different number of control sections as described by Coleman and Spacone [7]. In the same work a solution to this problem is proposed by introducing a constant fracture energy regularization technique. Later, a more robust solution was given by Scott and Fenves [8], where a new constant length plastic hinge integration method based on the modified Gauss–Radau quadrature was developed.

Recently Triantafyllou and Koumousis [9, 10] proposed a beam element, based either on Euler or Timoshenko theory, which treats material non-linearity at the elemental level through proper implementation of the Bouc-Wen hysteretic rule. Herein, the same approach is extended to incorporate a displacement based fibre beam element formulation suggesting also an efficient numerical procedure that treats hysteresis explicitly. Fibre stresses are decomposed into an elastic and hysteretic part that evolves on the basis of Bouc-Wen type evolution equation. This separation leads to global decomposition of internal forces into elastic and hysteretic ones which are then introduced to the equations of motion. The solution is derived numerically by updating the load vector and solving a system of linear equations using the Newmark method.

2 Formulation of the proposed element

Along the lines of the well-established distributed plasticity fibre elements, a frame structure is subdivided and analysed in three levels: the structural level, the elemental level and the cross-sectional level. The global structural equations of motion are formulated incorporating each element's contribution following the direct stiffness method. The beam element is considered as a fully bonded bundle of fibres forming a constant cross section that deforms on the basis of the assumption that plane sections remain plane after deformation. To account for a robust state determination of the element, namely its stiffness and internal forces, the element is discretized into a number of cross sections along its length. Further discretization of these cross sections into longitudinal fibres is an efficient way to describe their constitutive behaviour on the basis of Euler- Bernoulli assumption. It should be clarified that structural nodes exist only in the positions of joints meaning that the inner discretization along the elements is meant only as an efficient computational scheme aiming at dealing with material non-linearities. In the proposed formulation the constitutive relation of the uniaxial behaviour of fibres is based on the Bouc-Wen hysteretic model that smoothly accounts for the transition from the linear elastic behaviour to a linear plastic behaviour. This formulation is easily extended to account for stiffness degradation, strength deterioration and pinching by introducing and tuning additional parameters on the basis of existing experimental data.

2.1 Uniaxial Hysteretic Behaviour

A mechanical uniaxial model can be established and is represented schematically in Figure 1.

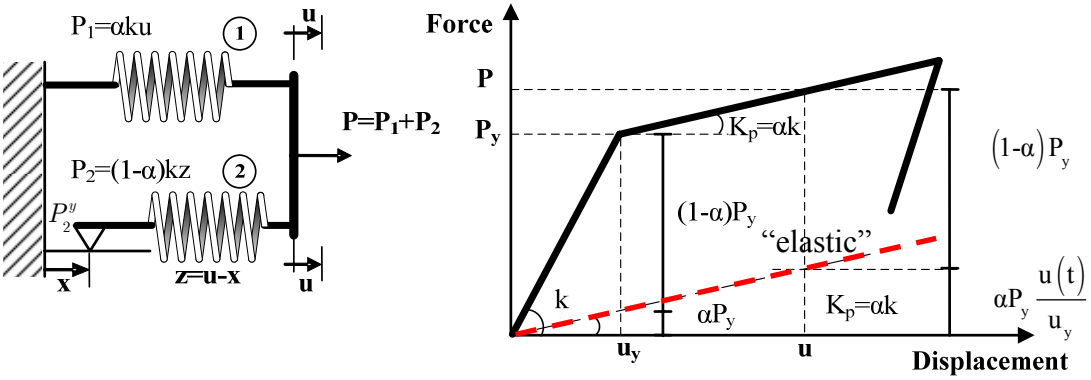

(a) (b)

Figure 1: (a) Bouc-Wen model components (b) Force-displacement relation

The model constitutes a parallel system of a linear spring (Spring 1) and a nonlinear element, as presented in Figure 1a. The nonlinear element consists of a linear spring (Spring 2) and a slider connected in series. Thus, a two degree of freedom system is considered with u, being the total displacement and z, the relative

displacement of Spring 2. From compatibility considerations, the sliding displacement, if any, is determined by the difference $(x = u - z)$.

As long as the force acting on the slider is smaller than a threshold value $\left(x_y\right)$, sliding does not occur and thus $x = 0$ while the relative displacement on Spring 2 is equal to the total imposed displacement. In such a case, the system behaves elastically with combined stiffness k, since springs 1 and 2 are given an elastic stiffness of $a \cdot k$ and $(1-a) \cdot k$ respectively, with a being the inelastic to elastic stiffness ratio.

When the slider threshold is overcome, sliding occurs and the relative displacement in spring 2 remains constant, denoted herein as z_y. All these phases are summarized in the following force-displacement relationship:

$$P_{res}^{BW} = P_1 + P_2 = \alpha k u + \left(1-\alpha\right) k z \tag{1}$$

where z is:

$$z = \begin{cases} u, & x \le x_y \\ z_y, & x > x_y \end{cases} \tag{2}$$

As in engineering applications, the internal variable x is neither easy to measure, nor derive theoretically, the total displacement at which sliding occurs is used to model the system. This can be easily derived (from a uniaxial tension experiment or by implementing a specific yield criterion).Thus relation (2) is expressed equivalently as:

$$z = \begin{cases} u, & u \le u_y \\ u_y, & u > u_y \end{cases} \tag{3}$$

Wen [11] proposed the following relation to smoothen the transition from the elastic (no sliding) to the inelastic response (sliding) of the system:

$$\dot{z}(t) = f(\dot{u}(t), z(t)) = \dot{u}\left[\mathrm{A} - h_1 h_2\right] \tag{4}$$

where:

$$h_1 = \left|\frac{z}{z_y}\right|^n, \qquad h_2 = \left(\beta + \gamma \operatorname{sgn}\left(z\dot{u}\right)\right) \tag{5}$$

h_1 can be regarded as a uniaxial flow rule and h_2 as the corresponding cyclic loading rate, while in the above relation, dot$(\cdot)$ denotes differentiation with respect to time.

Parameter n controls the smoothness of the transition from the elastic to the inelastic regime, while the terms β and γ, introduced in relation (5), are factors that affect the shape of the hysteresis loop (Sivaselvan & Reinhorn [12]).

2.2 Cross sectional discretization

Every cross section of an arbitrary shape is discretized in a number of fibres each having the properties of the corresponding material. In Figure 2 a reinforced concrete cross section consisting of fibres describing concrete and four reinforcing steel fibres is presented. Such modelling, by incorporating realistic stress-strains material relations, is an efficient way to calculate the stress field and the stress resultants of the cross section when subjected in a combined biaxial bending and axial loading. Hence, fibre models have been widely used for the calculation of moment curvature diagrams and failure surfaces of cross sections [13].

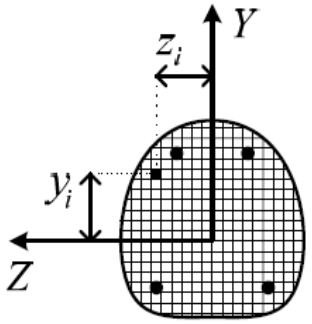

Figure 2: Cross sectional fibre discretization.

Based on the Euler-Bernoulli assumption that plane sections before deformation remain plane after deformation, axial deformation in every fibre can be calculated from the axial deformation and the two curvatures with respect to axes Y, Z at the centroid as:

$$\varepsilon(y,z) = \varepsilon_0 - y \cdot \varphi_Z + z \cdot \varphi_Y \tag{6}$$

The uniaxial stress in every fibre can be decomposed in an elastic and hysteretic part and is expressed accordingly as follows:

$$\sigma = \alpha_i \cdot \sigma^{el} + (1-\alpha_i) \cdot \sigma^h \tag{7}$$

where α_i is the post yield to elastic stiffness ratio of the fibre's material, σ^{el} is the elastic part expressed as $\sigma^{el} = E_i \cdot \varepsilon$ for the i material and σ^h is the hysteretic part. The same equation can be written in terms of deformations and the uniaxial stress-strain relation becomes:

$$\sigma = \alpha_i \cdot E_i \cdot \varepsilon + (1-\alpha_i) \cdot E_i \cdot z \tag{8}$$

where z is the hysteretic axial deformation of the fibre representing material i which depends on the total deformation ε and evolves according to the Bouc-Wen rule following the nonlinear differential equation:

$$\dot{z}(t) = \left[1 - \left| \frac{z(t)}{z_y^i} \right|^n \left(\beta_i + \gamma_i \cdot \mathrm{sgn}\left(z(t) \cdot \dot{\varepsilon} \right) \right) \right] \cdot \dot{\varepsilon} \tag{9}$$

Having already defined the expression of stress in every fibre, integration across the cross sectional area gives the stress resultants reactions of the section. So, in the case of a 2D beam the axial force and the moment are given as follows:

$$N = \iint_A \sigma dA \tag{10}$$

$$M = -\iint_A \sigma \cdot y dA \tag{11}$$

Replacing Equations (6) and (8) in the above relations and approximating the integrals as sums of every fibre contribution, the vector of the cross sectional forces $\{D\}$ at the centroid is given as:

$$\begin{Bmatrix} N \\ M \end{Bmatrix} = \begin{bmatrix} 1 & \cdots & 1 \\ -y_1 & \cdots & -y_n \end{bmatrix} \cdot \begin{bmatrix} a_i \cdot E_i \cdot A_1 & 0 & 0 \\ 0 & \ddots & 0 \\ 0 & 0 & a_i \cdot E_i \cdot A_n \end{bmatrix} \begin{bmatrix} 1 & -y_1 \\ \vdots & \vdots \\ 1 & -y_n \end{bmatrix} \cdot \begin{Bmatrix} \varepsilon_0 \\ \varphi_z \end{Bmatrix} + \ldots$$
$$+ \ldots \begin{bmatrix} 1 & \cdots & 1 \\ -y_1 & \cdots & -y_n \end{bmatrix} \cdot \begin{bmatrix} (1-a_i) \cdot E_i \cdot A_1 & 0 & 0 \\ 0 & \ddots & 0 \\ 0 & 0 & (1-a_i) \cdot E_i \cdot A_n \end{bmatrix} \cdot \begin{Bmatrix} z_1 \\ \vdots \\ z_n \end{Bmatrix} \tag{12}$$

$$\{D\} = [l]^T \cdot \left[C_{el} \right] \cdot [l] \cdot \{d\} + [l]^T \cdot \left[C_h \right] \cdot \{z\} \tag{13}$$

where $[l]$ is the geometrical matrix of the fibres position in the cross section, $\left[C_{el} \right]$ is the elasticity matrix of the cross section that corresponds to the post yield to elastic stiffness ratio a and $\left[C_h \right]$ is the hysteretic cross sectional constitutive matrix.

Having the cross sectional reactions decomposed into an elastic and hysteretic part, the elastic stiffness matrix $\left[k_{el} \right]$ of the element is derived. Also, the hysteretic

internal forces $\{p_{hys}\}$ are evaluated, while their integration along the beam's length gives the element's hysteretic end actions as it is described in the following section. This results into the following equation at the cross sectional level:

$$\{D\} = [k_{el}] \cdot \{d\} + \{p_{hys}\} \tag{14}$$

2.3 Element formulation

A 2D beam element with positive elastic and hysteretic end actions specified in Fig. 3 is considered.

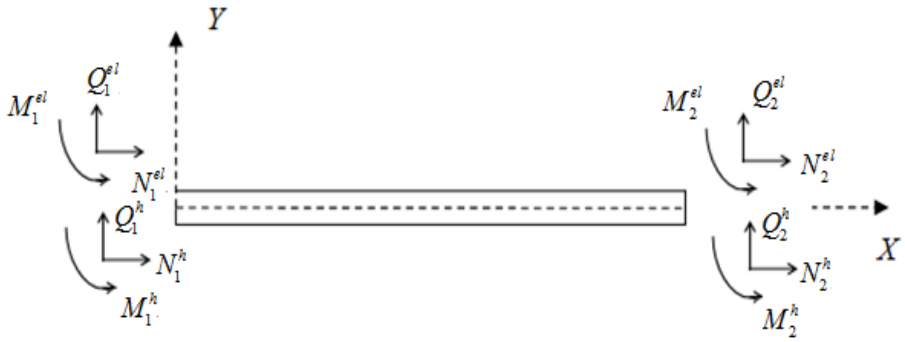

Figure 3: Degrees of freedom of the hysteretic element

An hysteretic beam element requires pairs of degrees of freedom, as in every physical one, an hysteretic component is added. This refers to a beam element state determination that consists of two parts. The first is the derivation of the elastic stiffness matrix as specified in the first part of Equation (14). The second is the derivation of the vector of hysteretic nodal elemental forces. These are performed using a deformation field which is expressed on the basis of cubic polynomial shape functions $[B]$ and the principle of virtual works considering Equation (14) as follows:

$$\int_0^L \{\delta d\}^T \cdot \left([k_{el}] \cdot \{d\} + \{p_{hys}\} \right) dx = \{\delta q\}^T \cdot \{Q\} \tag{15}$$

where $\{Q\}$ is the vector of total element nodal forces and $\{q\}$ the vector of nodal displacements. It results that the total nodal forces can be decomposed into their elastic and hysteretic parts, meaning that both these two states can be treated separately. Hence, the elastic element stiffness matrix is calculated using relation (16) and the nodal hysteretic forces are calculated from relation (17) as follows:

$$\left[K_{el}\right] = \int_0^L \left[B\right]^T \cdot \left[k_{el}\right] \cdot \left[B\right] dx \tag{16}$$

$$\left\{P_{hys}\right\} = \int_0^L \left[B\right]^T \cdot \left\{p_{hys}\right\} dx \tag{17}$$

The integrations are performed numerically according to the Gauss-Lobatto quadrature rule and the element is divided in a number of control sections as shown in Figure 4. This quadrature rule is more appropriate as it includes in the numerical scheme the two cross sections at the element's ends where the largest plastic deformations occur.

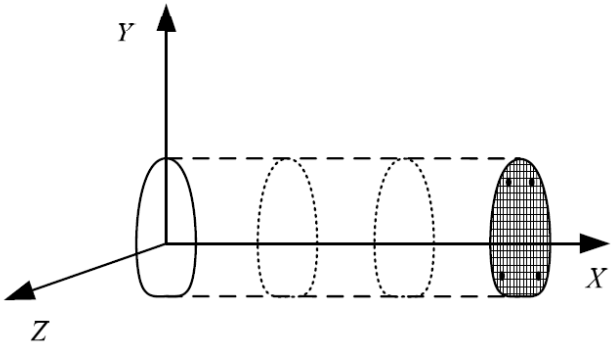

Figure 4: Control sections and fibres subdivision of the member.

2.4 System's equations of motion and analysis steps

For a multi degree of freedom structure, dynamic equilibrium can be established in terms of nodal displacements, velocities and accelerations as follows:

$$\left[M_S\right] \cdot \left\{\ddot{U}\right\} + \left[C_S\right] \cdot \left\{\dot{U}\right\} + \left\{P_{\text{int}}\right\} = \left\{P(t)\right\} \tag{18}$$

where $\left[M_S\right], \left[C_S\right]$ are the total mass and damping matrices and $\left\{P_{\text{int}}\right\}$ is the vector of internal nodal forces. Using Equations (16) and (17) at the element level and by assembling the matrices and vectors at the structural level, the above equation is written in the following form:

$$\left[M_S\right] \cdot \left\{\ddot{U}\right\} + \left[C_S\right] \cdot \left\{\dot{U}\right\} + \left[K_S\right] \cdot \left\{U\right\} = \left\{P(t)\right\} - \left\{P_{HYS}\right\} \tag{19}$$

where $\left[K_S\right]$, $\left\{P_{HYS}\right\}$ are the structure's elastic matrix and hysteretic forces vector respectively. Equation (19) can be solved by any numerical time integration scheme as for example the Newmark method. An interesting feature of the present formulation is that the elastic stiffness matrix is formed at the beginning of the marching process and remains constant throughout the entire analysis. The elastoplastic behaviour is introduced by the vector of hysteretic forces which is updated at every time step reducing the external loads according to the level of plasticity spreading.

All the necessary steps that constitute the procedure of the proposed formulation are summarized as follows:

1) Initial calculations: Formulate global matrices $\left[M_S\right],\left[C_S\right],\left[K_S\right]$ and start Newmark procedure.

In every time step of the Newmark method perform the following calculations:

2) From the known nodal velocity vector $\left\{\dot{U}\right\}$ calculate the rate of the axial deformation $\dot{\varepsilon}_0$ and the rate of curvature $\dot{\varphi}_Z$ in the centroidal axes of the control sections of every element.

$$\begin{bmatrix}\dot{\varepsilon}_0\\ \dot{\varphi}_Z\end{bmatrix}=\left[B\right]\cdot\left\{\dot{U}\right\} \tag{20}$$

3) On the basis of the Euler-Bernoulli assumption calculate the axial deformation in every fibre of the control section: $\varepsilon_{fib}=\varepsilon_0-y\cdot\varphi_Z$.

4) Solve Equation (9) for every fibre that gives the new hysteretic deformation.

5) Calculate the updated cross sectional hysteretic forces $\left\{p_{hys}\right\}$ according to the second part of Equations (13) and (14).

6) Integrate the cross sectional hysteretic forces along every element to derive the elemental nodal hysteretic forces $\left\{P_{hys}\right\}$ as indicated in Equation (17).

7) Assemble hysteretic forces vectors according to the contribution of every element, impose boundary conditions and form the total vector of the nodal hysteretic forces $\left\{P_{HYS}\right\}$.

8) Finally, correct the external load vector at the current time step by subtracting the nodal hysteretic forces and proceed with Newmark method calculations within the time step.

3 Numerical examples

The proposed element is compared with the displacement based fibre element of the Opensees software [14]. In all the analysis only material non-linearity is considered although the proposed model can also be extended easily to incorporate geometrical non-linearities. First, a steel cantilever column with IPE300 cross section is pushed laterally until major plastic deformations occur. The steel stress-strain law is considered bilinear with 2% hardening ratio and the Bouc-Wen parameters are set to $\alpha = 0.02$ and $n = 25$. The full Newton Raphson scheme with displacement control was utilized in Opensees to achieve convergence by imposing a displacement increment of $0.001\,m$. In the case of a doubly symmetrical beam and a plane frame problem, strips are replacing the fibres as uniaxial bending is developed. Hence, 25 total strips, 4 in every flange and 17 in the web were considered to discretize the IPE300 cross section as presented in Figure 5. Also, 5 integration points were considered along cantilever's length. The two static non-linear curves for both cases are presented in Figure 6.

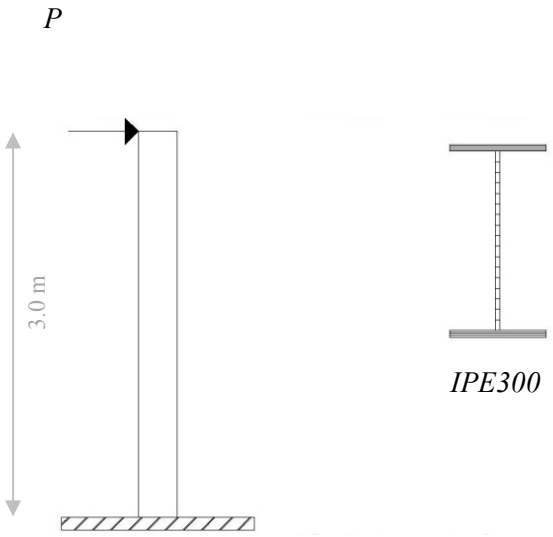

Steel properties	
E (KN/m^2)	210000000
f_y (KN/m^2)	235000
Bouc-Wen parameters	
n	25
β	0.5
γ	0.5

Figure 5: Steel cantilever column and cross section discretization

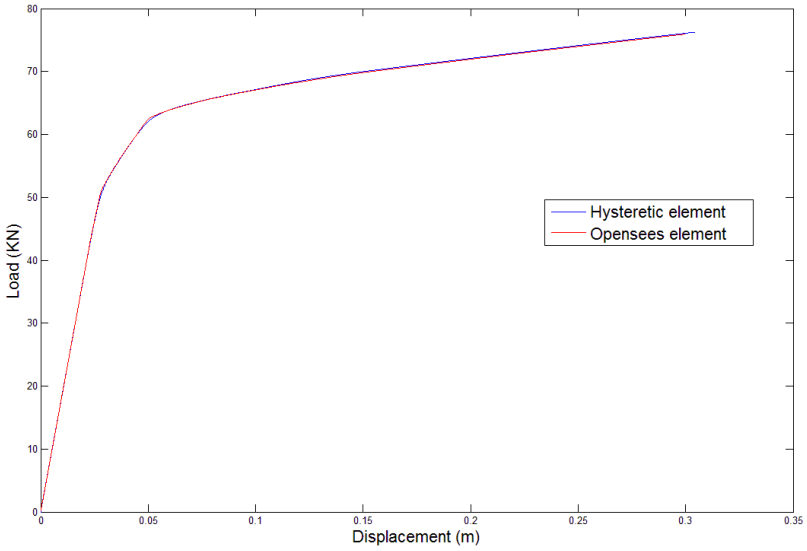

Figure 6: Static pushover curves for the steel cantilever

It is evident that the two curves are practically identical. This verifies that the proposed formulation is as accurate as the one of Opensees despite of the differences in the inelastic modelling between the two methods. Spreading of plasticity along the height of the cross section at the fixed end, at three different loading levels and the decomposition of the total stresses to the elastic and hysteretic part are depicted in Figure 7.

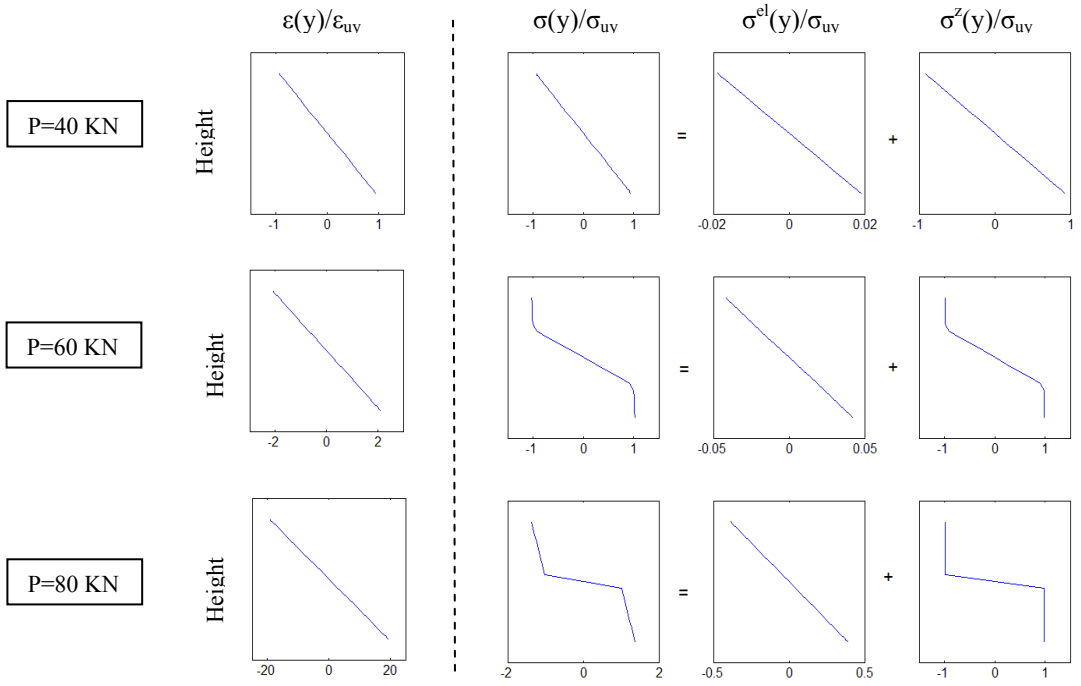

Figure 7: Deformations and stresses along the cross section's height

In the next example a reinforced concrete plane frame is analysed subjected to a monotonically increasing lateral load. All members are from the same rectangular 0.60x0.30 (m^2) cross section which is discretized in fibres, were each steel rebar is modelled by one fibre with equal area. The properties of the materials along with their Bouc-Wen parameters are presented in the Figure 8. Concrete is considered as elastic perfectly plastic, while steel has a hardening ratio of $a = 0.02$. Along every element 5 control sections are considered and for the cross section modelling 25 fibres were used in total, from which 4 represent the steel reinforcement.

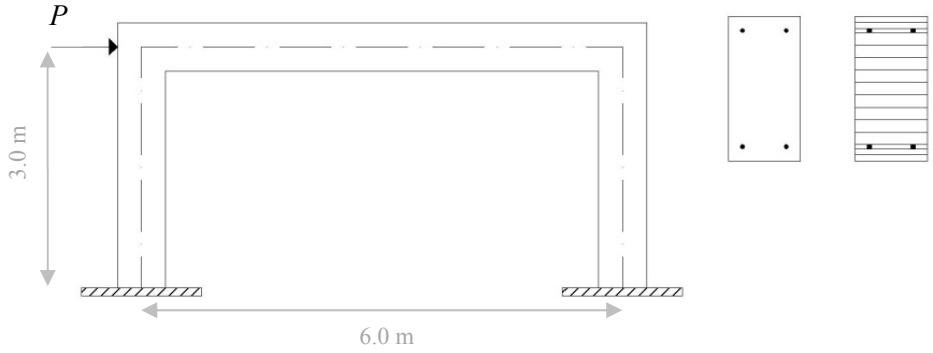

Steel properties	
E (KN/m^2)	210000000
f_y (KN/m^2)	500000
n	25
β	0.5
γ	0.5
Concrete properties	
E (KN/m^2)	30000000
f_y (KN/m^2)	20000
n	25
β	0.5
γ	0.5

Figure 8: Concrete frame and cross sectional properties

The nonlinear static pushover curves are presented in Figure 9 from which satisfactory agreement is demonstrated with the two solutions yielding almost the same result. From a closer evaluation, it results that both models predict the same point of initial yield and they terminate with the same post yield stiffness ratio, with the hysteretic model appearing to have a smoother transition from the elastic to fully plastic region.

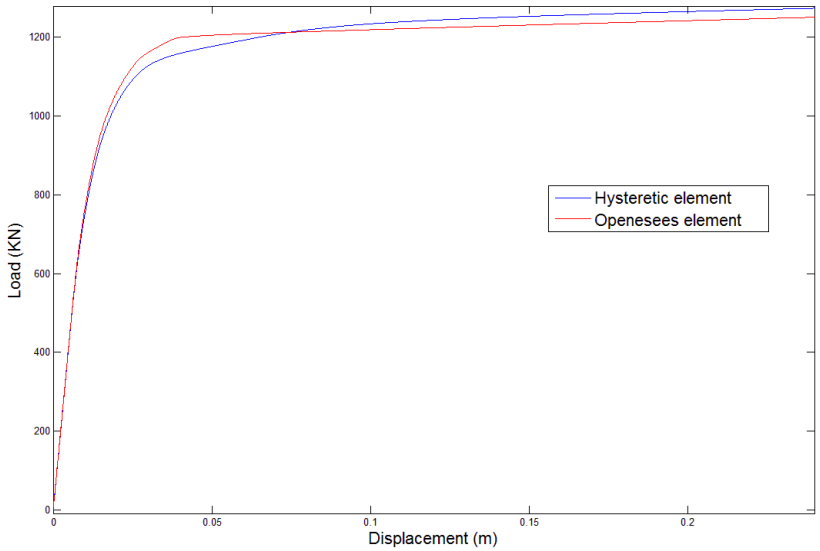

Figure 9: Static pushover curves of the RC frame.

In Figure 10 the base moment of the left column is presented together with the elastic and hysteretic components of the Bouc-Wen formulation. In the example, this elastic part is due to the steel only, as the concrete material was considered elastic-perfectly plastic, while in the hysteretic part both steel and concrete fibres contribute.

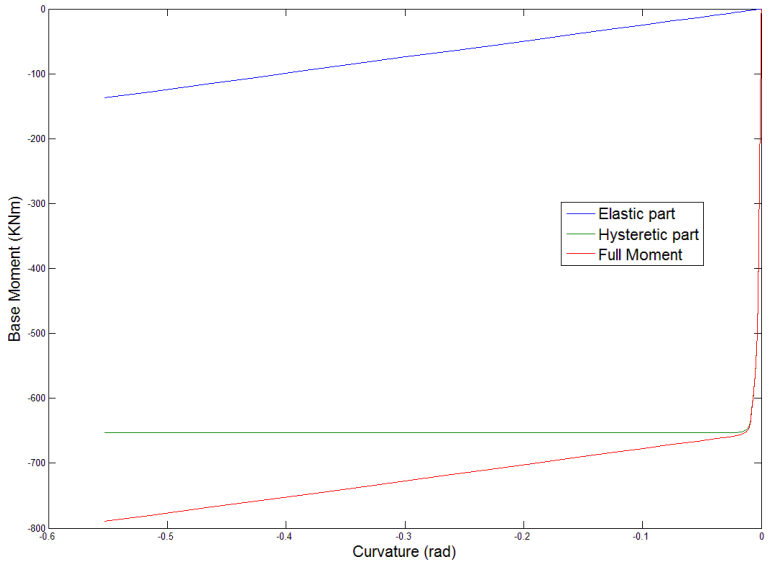

Figure 10: Elastic, hysteretic and full moment-curvature diagrams at the bottom cross section of the left column.

In the last example, a dynamic analysis is performed for the plane frame of the previous example but this time it has a steel IPE300 cross section. The imposed

loading is a sinusoidal load time history at the upper free nodes given by relation $P(t) = 130 \cdot \sin(5 \cdot t)$. The cross section is discretized into 50 fibres/strips along height and 5 control sections were selected along every element's length for the Gauss-Lobbato integration scheme. The displacement time history of the column-beam joint along with the result from the Seismostruct software [15] is presented in Figure 11.

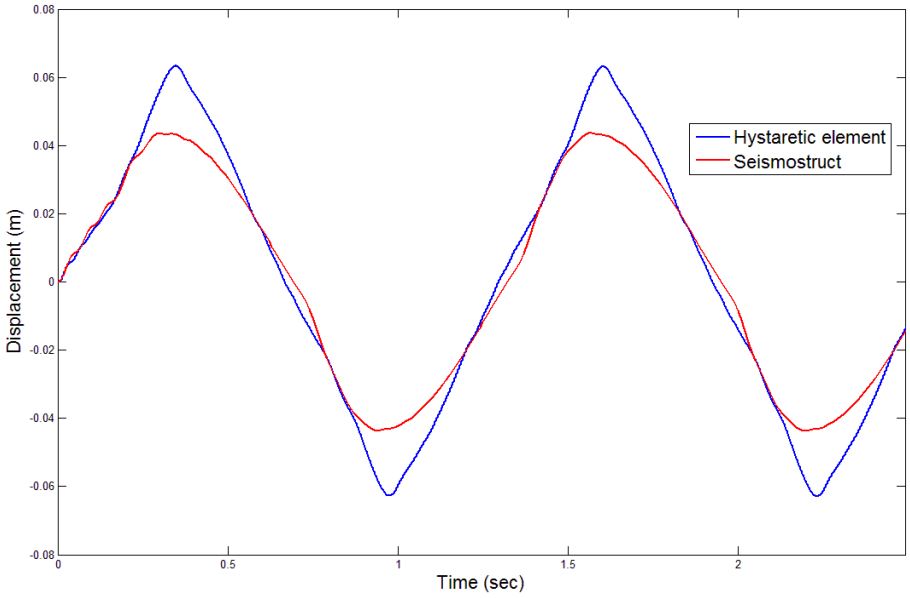

Figure 11: Displacement time history result of the free node.

The differences in the peak response are due to the fact that Seismostruct does not have the possibility to include internal control sections in the displacement based formulation. Consequently, plastic behaviour is restricted only at the two ends of each member making the structure stiffer, thus the ultimate displacements are reduced.

Along with the global response of the frame, the stress-strain plot of the outer fibre in the base of the frame's left column is presented in Figure 12. The total stress is the sum of the elastic one, which offers the hardening behaviour and the hysteretic one, which offers the elastoplastic behaviour. The shape of the hysteretic loop indicates the values of the Bouc-Wen parameters that were selected, namely n, β, γ. The large value of parameter n causes the loop to have almost sharp transition between the linear segments. On the other hand, the equal values of β, γ $(\beta = \gamma = 0.5)$ make the unloading branch parallel to the elastic one.

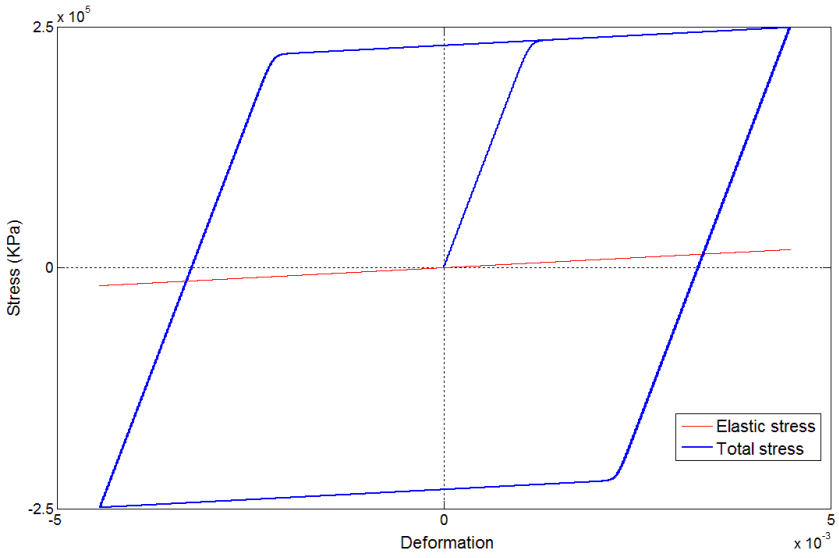

Figure 12: Stress-strain hysteretic loop of the outer fibre at the column.

It is also interesting to plot the stress distribution along the height of the same cross section in different instances of loading and unloading phases. Hence, in Figure 13 such evolution of stresses along the cross sectional height is presented. It is clear that when the load is reversing, external fibres unload first and they are reaching gradually their opposite sign yielding point as the load increases.

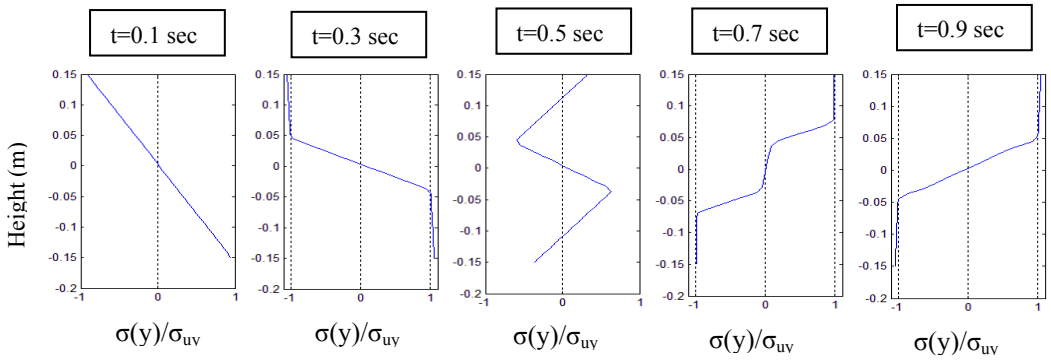

Figure 13: Stress distribution along the cross sectional height in different loading instances.

4 Concluding remarks

A fibre displacement based beam element with uniaxial, elastoplastic behaviour, governed by the Bouc-Wen model is proved quite efficient in performing the static and dynamic analysis of frame structures. The ability of the proposed formulation to model the hysteretic phenomena explicitly at cross-sectional, elemental and structural levels, facilitates considerably the solution, as it results into a set of linear

equations and the non-linearity of the system is reflected into the loading term. Bouc-Wen model can be easily extended to incorporate degrading phenomena enabling more realistic descriptions of structural behaviour.

From the numerical results presented, the validity and efficiency of the proposed approach is demonstrated and the interesting features of fibre modelling analysis that reveals the inner aspects of stress distribution within the section are manifested. This is of particular interest when more complex asymmetrical sections are considered, where the differences are usually more pronounced.

References

[1] Clough R. W., Benuska K. L. and Wilson E. L. "Inelastic earthquake response of tall buildings." Proc., 3rd World Conf. on Earthquake Engineering, Wellington, New Zealand, 1965.

[2] Giberson, M. F. "The response of nonlinear multistory structures subjected to earthquake excitation." PhD thesis, California Institute of Technology, Pasadena, Calif., 1967.

[3] Spacone E., Filippou F. C. and Taucer, F. F ''Fibre beamcolumn model for nonlinear analysis of R/C frames. I: Formulation.'' Earthquake Engrg. and Struct. Dyn., 25(7), 711–725, 1996.

[4] Bathe K.J. " Finite Element Procedures" , Prentice Hall Engineering, Science, Mathematics, New York, 2007.

[5] Spacone E., Ciampi V. and Filippou F. C. "Mixed formulation of nonlinear beam finite element." Comput. Struct., 58, 71–83, 1996.

[6] Neuenhofer A. and Filippou F. C. "Evaluation of nonlinear frame finite-element models." J. Struct. Eng., 123_7_, 958–966, 1997.

[7] Coleman J. and Spacone E. "Localization issues in force-based frame elements." J. Struct. Eng., 127_11_, 1257–1265, 2001.

[8] M.H. Scott and G.L. Fenves "Plastic Hinge Integration Methods for Force-Based Beam–Column Elements." Journal of Structural Engineering © ASCE, February 2006.

[9] S. Triantafyllou and V. Koumousis, "Small and Large Displacement Dynamic Analysis of Frame Structures Based on Hysteretic beam Elements" Journal Of Engineering Mechanics, Volume 138, Issue 1, Pages 36-49, July 2011.

[10] S. Triantafyllou and V. Koumousis, "An inelastic Timoshenko beam element with axial-shear flexural interaction" Computational Mechanics, Volume 48, Issue 6, Pages 713-727, December 2011.

[11] Wen, Y.K., "Method of random vibration of hysteretic systems", Journal of Engineering Mechanics Division, 102, pp. 249-263, 1976.

[12] Sivaselvan M. V., Reinhorn A. M. Hysteretic Models for deteriorating inelastic structures, Journal of Engineering Mechanics 126 (6), pp. 633-640, 2000.

[13] A.E. Charalampakis, V.K. Koumousis, "Ultimate strength analysis of composite sections under biaxial bending and axial load" Advances in Engineering Software, 39, 923–936, 2008.

[14] McKenna F., Fenves G., Scott, M.: “Open system for earthquake engineering simulation”. University of California, 2000.
[15] SeismoSoft. 2006. SeismoStruct- A Computer Program for Static and Dynamic Nonlinear Analysis of Framed Structures, Available online at http://www.seismosoft.com.
[16] Bouc R., (1967). “Forced vibration of mechanical systems with hysteresis”, Proceedings of the Fourth Conference on Non-linear oscillation, Prague, Czechoslovakia.